Rayleigh-Taylor Instability with varying periods of zero acceleration

Denis Aslangil
Member of ASME
Post Doctoral Associate, Computational Physics and Methods, CCS-2
Los Alamos National Laboratory, Los Alamos, New Mexico 87545 USA
Email: denis.aslangil@gmail.com

Zachary Farley
Ph.D. Student, Department of Mechanical Engineering & Mechanics
Lehigh University, Bethlehem, Pennsylvania 18015 USA
Email: zkf216@lehigh.edu

Andrew G.W. Lawrie
Lecturer, Hele-Shaw Laboratory, Queen's Building
University of Bristol, Clifton BS8 1TR UK
Email: Andrew.Lawrie@bristol.ac.uk

Arindam Banerjee *
Member of ASME
Professor, Department of Mechanical Engineering & Mechanics
Lehigh University, Bethlehem, Pennsylvania 18015 USA
Email: arb612@lehigh.edu

*Address all correspondence for to this author.

ABSTRACT

We present our findings from a numerical investigation of the acceleration-driven Rayleigh-Taylor Instability, modulated by varying periods without an applied acceleration field. It is well known from studies on shock-driven Richtmyer-Meshkov instability that mixing without external forcing grows with a scaling exponent as $\approx t^{0.20-0.28}$*. When the Rayleigh-Taylor Instability is subjected to varying periods of "zero" acceleration, the structural changes to the mixing layer remain remarkably small. After the acceleration is re-applied, the mixing layer quickly resumes the profile of development it would have had if there had been no intermission. This behaviour contrasts in particular with the strong sensitivity that is found to other variable acceleration profiles examined previously in the literature.*

1 INTRODUCTION

The Rayleigh-Taylor instability (RTI) develops at the interface between two fluids with differing densities ρ_h and ρ_l that are subjected to an external acceleration field, g [1, 2]. Perturbations to the interface develop, for a miscible fluid, into a layer of energetic turbulent mixing dominated by emergent interpenetrating vortical structures that lies between layers of unmixed fluid. Classical RTI, where g is not a function of time (t), has been extensively studied, see comprehensive reviews by [3, 4]. The instability has much slower long-term growth than exponential, and is typically characterized [5] by:

$$h_{b,s} = \alpha_{b,s} A g t^2, \tag{1}$$

where $h_{b,s}$ is a width of thickness of the mixing layer, the Atwood number $A = \frac{\rho_h - \rho_l}{\rho_h + \rho_l}$ is a non-dimensional density difference, g is the acceleration and t is the time. In flows with moderate and high Atwood numbers ($A > 0.1$), we distinguish between rising and falling structures by introducing h_b denoting bubbles, i.e. plumes of light fluid rising through the heavier fluid; and h_s denoting spikes of heavy fluid falling through the lighter fluid. At low Atwood numbers, the mixing layer is symmetric, however, with large differences in density, spikes develop more rapidly [6–9].

RTI is found in many energetic processes including combustion and chemically reacting flows, in our polar oceans underneath sea ice and within weather inversions. Besides, on astronomical timescales it occurs within Type-1a supernovae and in certain geological processes associated with volcanic activity over viscous time scales (see [9–14]). However, in the astrophysical context (e.g. [15]) and in some engineering applications (e.g. inertial confinement fusion [16]) the configuration is typically $g(t) \neq \text{const}$, indicating that hydrodynamic instabilities are driven by a time-dependent externally applied accel-

eration field. Such flows remain a great challenge for models, most of which rely on an assumption of Fickian diffusion and often fail to capture rapid locally and temporally varying changes in the generation of turbulence from instability driven forces. As a result, increasing attention has been given in recent years to Rayleigh-Taylor instability undergoing variable acceleration (see, in particular, [17–23]).

Until now, most work on variable acceleration in RTI has followed the time-histories known as accel-decel-accel or "ADA" [19] where periods of acceleration is followed by periods of acceleration reversal or deceleration. Dimonte and Schneider [17] was the first to examine RTI over a range of acceleration histories applied to an immiscible fluid pair, Freon and water ($A = 0.22$). Subsequent work compared Implicit Large Eddy Simulations (ILES) [24] with previously unpublished experimental results ($A = 0.48$) [25] and it was concluded that ILES with a broadband initial perturbation spectrum matched the experiments. Some more recent work has focused on the sensitivity of future development to initial conditions, [21], and has found that structural features of the initial condition persist through to the second acceleration. Another recent study also examined the sensitivity to duration of deceleration [23]. This behavior is consistent with [18], and more recently, a number of studies have considered repeated cycling between acceleration and deceleration, as reported in [22].

In recent studies using the more abstract Homogenous Variable-Density Turbulence (HVDT), where the flow is configured so that mixing occupies the entire domain, sharp changes in acceleration have been explored for the cases of acceleration reversal and removal [20]. There, bubble and spike features specific to the periphery of an RTI mixing layer are no longer present, and the configuration is representative of the flow deep in the interior of a variable-density mixing layers. In the case that acceleration ceases after an initial period, the authors reported that the loss of baroclinically generated large-scale motion led to a decay in the rate of mixing and a rapid decrease in turbulence

intensity [26].In addition, recent work HVDT has been used to study structural changes to variable density turbulence when turbulent kinetic energy evolution is highly nonlinear. In HVDT under constant acceleration, a smooth transition from rapidly increasing to gradually decaying variable-density turbulence was observed that may be expected to persist in the more general case of RTI with constant- and variable-acceleration profiles with smoother transitions, and different variable-density flows such as RMI, mixing layers and jet flows [26–28].

The behavior of RTI undergoing ADA tends to be dominated by peripheral structures, particularly during the deceleration phase [21]. Here, there is no further growth of the mixing layer, yet the layer continues to mix, collapsing the distribution of densities within the layer. Subsequent re-acceleration may be compared with the classical RTI problem that commences with an unusually thick interface and a substantial fraction of total energy held as kinetic energy inside the mixing layer. The response to the acceleration reversal strongly depends on the spectral content of these conditions at the moment of re-initialization. Asymptotically, self-similar evolution is recovered (see [21, 29]), but we discovered in recent work, [23], that in the short term, re-growth of RTI is sensitive to the proportion of kinetic energy where the vertical component dominates, and this is attributed to internal wave activity within the mixing layer.

In the present study, we consider the special case where there the applied acceleration is completely withdrawn or ”zero” for some duration in the evolution. We call this profile “AZ”. This is closely related to the Richtmyer-Meshkov Instability (RMI) [30, 31], where a mixing layer evolves with no external forcing after an initial injection of vorticity at the interface, usually provided by transmission of a shock through it. Our configuration differs, in principle, only by the mechanism of the initial acceleration. Here, buoyancy-forces over a longer period of time generate vorticity on the interface.

The rest of the paper is organized as follows. In §2 we describe the numerical methods

used to integrate the variable-density conservation statements. The initial conditions are discussed in §2.1. In §3 we draw the connection between RMI and our modification to the classical RTI. We also show that the structural composition of an AZ flow contrasts with a previously studied counterpart, "AD" where we apply an indefinite period of deceleration. The AZ configuration is a necessary precursor to better understand subsequently re-acceleration, a case we introduce here as "AZA". We study the RM limit in §3.1, and examine its growth in §3.1.1. We then report the evolution of second order moments in §3.1.2 before considering re-initialized acceleration, that we term "AZA" in §3.2. Finally, we summarize our findings in §4.

2 METHODS

Simulations reported in this study were performed using MOBILE, a distributed memory, variable density, pressure-correction incompressible Eulerian flow solver. It uses an Implicit Large Eddy Simulation (ILES) methodology to dissipate excess energy from the mesh scale. MOBILE has been validated across a broad range of systems that involve mixing and transport, including single-mode and multi-mode Rayleigh-Taylor flows up to Atwood A = 0.9 [29, 32], jet flows with background flows [33, 34], Kelvin-Helmholtz Instability [35], lock-release gravity currents [35], systems with unusual geometries [36, 37], and systems undergoing variable acceleration [19, 21]. Mass and momentum are advected within a finite volume framework, and a fractional step approach decouples hyperbolic (advective transport), parabolic (viscous dissipation and scalar diffusion), and elliptic (pressure/velocity correction) components. Following from the work of [5] and [24], MOBILE performs a sequence of total-variation-bounded one-dimensional advection subproblems that eliminate spurious oscillations around steep material gradients. Additional algorithmic details are documented elsewhere e.g. [35].

2.1 Acceleration profiles, problem setup, and initial conditions

Three different acceleration profiles are examined in this study:

(i) CG: classical RTI where the acceleration remains constant during the whole flow evolution,

(ii) AZ: configuration where the RTI begins like case (i) until applied acceleration is removed, and

(iii) AZA: a sequence of configurations that follow the acceleration profile of (ii) until the acceleration is re-applied.

We investigate the behaviour of the instability with a varying range of "Z" durations for which acceleration has been removed and compare it with the AZ and the CG cases. The AZ case,(ii), is related to RMI because in both cases, the variable-density mixing layer grows under the absence of the external forcing using momentum from some form of imposition of vorticity on the interface. Typically in experiments this is applied by transmitting a shock through the density interface. but equally an impulsively applied external field of acceleration also generates the key behaviour [17, 38]. In the limit of short RTI development and a long period of no acceleration, it is conjectured that the key features of these flows will be asymptotically similar.

Table 1 lists the acceleration profile for all the cases investigated in this study, a representative AZA profiles is shown in figure 1 . For all AZ and AZA cases, the first acceleration change occurs at $t = 2s$, to remain consistent with the preceding literature [19, 21], and selects a time when the flow has already established self-similar development. The AZA1 and AZA2 cases listed in the table are motivated by the authors recent work [23], where it is shown that the growth of the mixing layer during re-acceleration phase is sensitive to the proportion of kinetic energy with a dominant component in the vertical direction. This sensitivity is attributed to the phase angle of internal gravity waves and the corresponding distribution of energy in the flow (see fig. 3, §3.1 and for more details [23]). The

AZA3 and AZA4 cases seek to investigate the effect of long-term removal of acceleration on re-growth during the second acceleration.

For all the cases examined in this paper, the domain has aspect ratio given by $L \times L \times 3L$, domain with the resolution of $256 \times 256 \times 768$. For ease of interpretation we set $L = 1cm$. The density of the pure heavy and light fluids are $\rho_h = 3\ g/cm^3$and $\rho_l = 1\ g/cm^3$, respectively. These densities lead to $A = (\rho_h - \rho_l)/(\rho_h + \rho_l) = 0.5$. The magnitude of the acceleration field is chosen as $-4\ cm^2/s$ to allow comparison with previous studies [19, 21]. The initial interface between the light and heavy fluids are perturbed as multi-mode annular initial-conditions as

$$h(x,y) = \sum_{k_x k_y} a_k \cos(k_x x)\cos(k_y y) + b_k \cos(k_x x)\sin(k_y y) + c_k \sin(k_x x)\cos(k_y y) + d_k \sin(k_x x)\sin(k_y y) \tag{2}$$

between the wave numbers 32 to 64 where the random amplitude coefficients are scaled to maintain the desired initial kinetic energy $\langle h_0'^2 \rangle/2 = \int_{k_{\min}}^{k_{\max}} E_{h_0}(k)dk = 3.15 \times 10^{-4} L$ [8,39].

3 RESULTS AND DISCUSSIONS

In this section, we examine the AZ and AZA configurations. As noted in the previous section, the AZ profile has strong similarities with RMI and in §3.1 we consider in particular the long-term behaviour of a mixing layer after acceleration has ceased. We then discuss in §3.2 how a period without acceleration affects the subsequent resumption of unstable development of the mixing layer when the acceleration resumes and we compare our findings with previously published work on ADA.

3.1 Effects of neutral (zero) acceleration

Here we consider the long-term behaviour of a mixing layer after acceleration has ceased, using integral statistics in §3.1.1 and second order statistical quantities in §3.1.2

to quantify the key indicators of self-similarity. The purpose is two-fold; the integral statistics gives us estimates of the global structure of the mixing layer; the higher-order turbulence statistics provides insight into momentum and energy transfer processes that play a significant role in these flows [8, 9, 21, 26].

3.1.1 Evolution of the growth parameters

Clear qualitative differences may be observed in figure 2 between the constant acceleration (CG), accel-decel (AD), and accel-zero (AZ) cases with a common annular initial condition. Two-dimensional vertical and horizontal planes of the density field at the center of our computational domain are plotted with a common time-origin (t = 4.5 s). The mixing layer width is greatest for classical RTI CG case, since its expansion has occurred continuously, whereas the other two cases have had an interruption to their expansion. In a decelerated flow (AD case), we have a restoring buoyancy force and the mixing layer is statically stable, and we found in [21] that it ceases to expand. The acceleration reversal shreds previously formed bubble and spike structures under a stabilizing deceleration phase, resulting in rapid mixing occurring in its interior.For the corresponding zero acceleration case of AZ, we observe that the mixing layer appears qualitatively similar to the CG case, even without a source of new kinetic energy (KE) to drive mixing layer expansion. However, it is remarkably distinct from the AD case. Dissipation of KE after acceleration ceases appears to induce fewer structural changes to the flow than a restoring buoyancy force. In addition, the mixing layer of the AZ case is longer than the AD case as the flow experiences slow expansion.

Some recent computational studies have shown that the mixing layer expands rapidly during acceleration and then shrinks slightly during deceleration, before resuming expansion under re-acceleration at a rate that is sensitive to the duration of deceleration [21,23]. We attribute the sensitivity to internal wave activity that occurs within the mixing layer,

producing an oscillatory exchange of kinetic energy (KE) and potential energy (PE). Depending on the mean phase angle of these waves at the moment of re-acceleration, the distribution of total energy in the mixing layer between KE and PE is highly variable and strongly influences the subsequent resumption of mixing layer expansion.

A quantity that acts as a well-filtered proxy for the response of the flow to acceleration and deceleration is the anisotropy tensor, B, a normalized, directional measurement of KE. B is the deviatoric part of the Reynolds stress tensor normalized by the KE. For isotropic turbulence, B_{11} = B_{22} = B_{33} = 0, and thus B = 0. More generally, -1/3 $\leq B \leq$ 2/3, where the upper and lower limits represent one-dimensional and two dimensional distributions of the KE [6]. Thus, B characterizes the geometry of turbulence and is independent of the amplitude of the fluctuations. For RTI, we are interested in the vertical component of B which is defined as

$$B_{33} = \frac{u_3 u_3}{u_i u_i} - \frac{1}{3}\delta_{ii}, \tag{3}$$

where the trace is removed so that the magnitude is zero in a perfectly isotropic flow. Figure 3 presents the evolution of B_{33} for CG, AZ and AD cases. The RTI CG case is highly anisotropic in the vertical direction, as a result $B_{33} > 0$; this finding is consistent with experimental measurements where values of B_{33} 0.2 is reported [9] with the value dropping to zero near the edges due to isotropy. For the AZ case, as the acceleration is withdrawn, we observe that B_{33} slowly decays towards zero as the mixing layer becomes progressively more isotropic. This observation is consistent with studies of RMI [40]. The AD case exhibits internal wave like behavior as the acceleration is reversed; the vertical component of the anisotropy tensor is observed to oscillate as shown in fig. 3. The amplitudes of these oscillations decrease as the deceleration phase continues as the flow

has regimes where the vertical direction of the velocity is highly anisotropic [23].

It is also of interest to consider a more flexible definition of the proportionality constant, $\alpha_{b,s}$, originally given in (1). A generalized definition,

$$\alpha_{b,s}(t) = \frac{\dot{h}_{b,s}^{\,2}}{4Agh_{b,s}}, \tag{4}$$

For the current analysis, we replace $h_{b,s}$ with the integral mix width W defined as [5, 41]:

$$W = 6\int_{-\infty}^{\infty} f_h(1-f_h)dz, \tag{5}$$

where f_h is the planar averaged volume fraction of the heavy fluid. The integral was taken over the entire domain that includes the mixing region such that the integral returns a zero value in the pure fluids. The factor of 6 derives from considering the width of the volume fraction (density) which is assumed to have a linear profile across the mix width [41]. Equation (4) was proposed by [6] using a self-similar analysis of small Atwood number RTI mixing. In the asymptotic limit of a classical CG RTI, a close to constant value of $\alpha_{b,s}$ is expected. This is widely taken as evidence of an invariance associated with self-similarity for experiments [9] and computations [7]. We expect a different form of a self-similarity during zero acceleration, but anticipate that the corresponding exponent will also tend to a constant value. We take the definition proposed in [42] for the development of the RMI as:

$$W(t) \approx (t-t_0)^{\theta}. \tag{6}$$

Due to the correspondence between RMI and our AZ case, the exponent θ is adopted as a key measure of mixing layer development after acceleration has ceased. The study of Weber et al. [42] covers a wide range of Atwood numbers (0.22 - 0.73), and Mach number (1.1 - 1.9) and present flow statistics for non-dimensional times ≈ 30 that is well beyond times reported in other RMI studies [3, 4].

Energy persisting in the flow after cessation of acceleration is converted relatively slowly by dissipation, so the mixing layer will continue to grow for the long term, until no kinetic energy remains. In this study we use an incompressible code, where the time step is limited by the fluid velocity and not by acoustic propagation making it possible to compute longer durations than most of the previous RMI studies. A recent collaborative effort on RMI [43] compared θ using various codes suggest a $\theta \approx 0.29$. However, Weber et al's [42] study shows convergence at much later normalized times (τ) > 25 and lower theta values. Note that slightly larger values from the theta group is at $\tau \approx 6$. This enables us to contribute to some long-standing questions [3, 4, 43] about the widely accepted self-similar scaling, θ, of mixing layer development under zero acceleration. We find that immediately after acceleration ceases, the mixing layer continues to expand rapidly for an initial period; shortly thereafter the expansion slows and it is the asymptotic self-similar behaviour, found after the transients have decayed, that is of particular interest here. We present in figure 4 our simulations, together with bounds $\theta = 0.2$ and $\theta = 0.28$ as reported by Weber [42] for various range of different initial conditions, and find that our results to be consistent with these expectations.

3.1.2 Evolution of the second order moments

We present in figure 5 the time-evolution of the second order moments of the velocity and scalar fields in the AZ case. After cessation of acceleration, both the normalized density-velocity correlation, $\frac{\langle u_3 c \rangle}{h^{0.5}}$, and the normalized vertical component of KE, $\frac{\langle u_3 u_3 \rangle}{h}$,

decays gradually as there is no production of KE in the mixing layer due to acceleration withdrawl. The KE that remains in the flow at the instant of acceleration withdrawl is dissipated over time. Moreover, along with the other velocity components, u_3 reduces progressively as the flow tends to become isotropic. We remark that the velocity-density correlation $\langle u_3 c \rangle$ decays more slowly than the $\langle u_3 u_3 \rangle$, and infer from this that the density fluctuations are less strongly affected by removal of acceleration than velocity fluctuations. This may be seen qualitatively in 2 and we infer that the density field preserves its structure more completely in the absence of acceleration.

An important statistical measure of the completeness of mixing, known as the molecular mixing parameter, Θ, is defined as

$$\Theta = \frac{\langle f_h f_l \rangle}{\langle f_h \rangle \langle f_l \rangle}, \tag{7}$$

where f_h and f_l are the mass fractions of the pure light and pure heavy fluids. In classical CG RTI, the asymptotic value of Θ is reported by [6, 8, 44] to fluctuate around the value of 0.7. The evolution of Θ is shown in figure 5(c) to vary only weakly in the constant acceleration (CG) configuration. This indicates we have already reached a self-similar state before any changes are made to the applied acceleration. We observe a small increase in Θ in our AZ case just after acceleration ceases, and we attribute this to a sudden decrease in our measure of vertical mass flux $u_3 \ c$ (see fig. 3.1.2 (b)). For both CG and AZ cases it is shown that Θ is invariant in the late time, once transients associated with the sudden cessation of acceleration have decayed away. However, the long-term value of Θ is also largely unaltered from that obtained in the self-similar limit of a RTI unstable, accelerated mixing layer. We may infer therefore that in the AZ case although mixing layer development is retarded without a continuous source of PE, vertical

mass fluxes are smaller and turbulence intensities are lower so we anticipate mixing will be reduced, nonetheless little has changed structurally. We might therefore expect any resumption of acceleration to drive mixing layer expansion that is largely independent of the duration of zero acceleration.

3.2 Rayleigh-Taylor instability under AZA profile

Previous work on RTI ADA with history has shown that during a statically stable deceleration, mixing takes place very rapidly [19, 21]. This decorrelates the bubble and spike structures and unmixed fluid ceases to inter-penetrate deep into the mixing layer. With subsequent resumption of acceleration we have established a strong sensitivity to the duration of preceding deceleration. However, as the following results will show, in the AZA configurations, we obtain a remarkable independence of mixing layer expansion rates with respect to the duration of zero acceleration once the acceleration resumes.

3.2.1 Evolution of the growth parameters

A qualitatively distinct behaviour can be first observed in figure 2(a), showing an AD case examined in [21], compared with our present AZ configuration shown in figure 2(b) at the same instant in time (t=4.5 s). Without a restoring force, there is no evidence that the spike and bubble structures in the RTI mixing layer decorrelate. However, an oscillatory exchange of KE and PE introduce sensitivity into the timing for resuming acceleration; the authors shown that variability in the subsequent rate of mixing layer expansion for an RTI ADA case may exceed 30% depending on the period of deceleration [23].

In the AZ case, the KE that remains after acceleration ceases sustains progressively less mixing but does nothing to impede mixing layer expansion once acceleration resumes. Since Θ preserved its value throughout both ‘A’ and ‘Z’ periods of an AZ configuration (see figure 5), we infer that the structure of the mixing layer is not substantially affected by varying periods of zero acceleration. We consider that its continued, albeit

slower, expansion is necessary to preserve its structural properties, and the evidence in figure 6 indicates clearly that growth rates during subsequent re-acceleration are indeed independent from the duration of zero acceleration. This interesting behaviour is in stark contrast to previously studied ADA configurations [19, 21, 29]).

3.2.2 Evolution of the second order moments

In this subsection, we investigate the behaviour of several second order moments of the flow during the second acceleration phase. As seen in figure 7(a), upon re-acceleration, the contribution of u_3u_3 to KE from vertical velocity quickly recovers its self-similar asymptotic value of ≈ 0.2. The mixing layer once again becomes highly anisotropic as conversion from PE to KE (see fig. 8) resumes and preferentially induces more rapid vertical motion. Once acceleration resumes, the average mass flux (velocity-density) correlation $u_3\ c$ shown in figure 7(b) increases transiently as RTI recovers and then stabilises. Conversely, Θ decreases slightly as shown in figure 7(c), and we attribute this to the transient increase in average mass-flux, since this corresponds to increased inter-penetration by unmixed fluid deep into the mixing layer. We remark that some limited variability does exist between the AZA cases, notable both in the duration of re-acceleration transients and in the degree to which fully-developed self-similarity is reached before the mixing layer expands to fill the simulation domain.

4 DISCUSSIONS AND CONCLUSIONS

The current study explores RTIr-induced mixing with variable periods of complete acceleration withdrawal. The acceleration is removed for either some intermediate (AZA) period or for some indefinite (AZ) period, the results are compared to the classical constant-gravity (CG) case. Our findings are summarised below.

In the AZ case the early ‘A’ stage is statistically identical to the classical RTI with mixing layer expansion scaling with t^2, but in the ‘Z’ stage we find strong parallels with

the shock-driven RMI. Here the kinetic energy progressively decays, but the mixing layer continues to expand, albeit much more slowly. The scaling behaviour of this expansion follows t^θ, and in this paper we obtain values of θ that lie in a range consistent with previous studies (e.g. [42]) on RMI. By using explicit incompressible simulations where numerical stability is limited by fluid advection velocities rather than acoustic propagation, then we can efficiently calculate long-term scaling in this decaying flow.

We compare the AZ case with the previously studied behavior of indefinite deceleration (AD) and we notice several important distinguishing features. In a decelerated flow we have a restoring buoyancy force and the mixing layer is statically stable, so it ceases to expand, despite rapid mixing occurring in its interior. One particular marker of internal structure is the vertical component of the anisotropy tensor, B_{33}, and we find whereas it oscillates in the AD configuration, for AZ cases there is simply progressive decay of anisotropy and it scales self-similarly with kinetic energy, once again consistent with studies of RMI. Our study of the AZ configuration has been a necessary precursor to examining AZA configurations. We varied the intermediate duration over which acceleration is not applied, and made the surprising discovery that subsequent mixing layer expansion is almost entirely unaffected by such periods. Layer expansion resumes at a rate that we show in this paper to be independent of the duration over which acceleration is removed. In particular this contrasts with our previous work on AD, where strong sensitivity is found. Here we present evidence obtained from second-order statistical quantities that there are few structural changes made to the mixing layer during the intermediate 'Z' stage, and in particular no decorrelation of existing bubble and spike structure that might impede the resumption of mixing layer expansion. Almost immediately, we find that the re-accelerated mixing layer is statistically indistinguishable from a classical self-similar RTI as growth resumes.

ACKNOWLEDGEMENTS

This article is dedicated to the memory of Malcolm J. Andrews who was a pioneer of several innovative experimental techniques of RTI and also developed a two-phase ILES code, RTI-3D [24] that has been used extensively by several researchers. Arindam Banerjee would also like to thank the U.S. National Science Foundation (Award No. 1453056) and DOE/NNSA SSAA Program (Grant No. DE-NA0003195) for financial support that made this work possible.

REFERENCES

[1] Rayleigh, L., 1884. "Investigation of the equilibrium of an incompressible heavy fluid of variable density". *Proceedings of Royal Society of London,* **14**, pp. 170–177.

[2] Taylor, G., 1950. "The instability of liquid surfaces when accelerated in a direction perpendicular to their planes i.". *Proceedings of Royal Society of London Series A,* **201**, pp. 192–196.

[3] Zhou, Y., 2017. "Rayleigh-Taylor and Richtmyer–Meshkov instability induced flow, turbulence, and mixing. i". *Physics Reports,* **720-722**, pp. 1–136.

[4] Zhou, Y., 2017. "Rayleigh-Taylor and Richtmyer–Meshkov instability induced flow, turbulence, and mixing. ii". *Physics Reports,* **723**, pp. 1–160.

[5] Youngs, D., 1984. "Numerical simulation of turbulent mixing by Rayleigh-Taylor instability". *Physica D: Nonlinear Phenomena,* **12**, pp. 32–44.

[6] Ristorcelli, J., and Clark, T., 2004. "Rayleigh-Taylor turbulence: self-similar analysis and direct numerical simulations.". *Journal of Fluid Mechanics,* **507**, pp. 213–253.

[7] Cabot, W., and Cook, A., 2006. "Reynolds number effects on Rayleigh-Taylor instability with possible implications for type-ia supernovae". *Nature Physics,* **2**, pp. 562–568.

[8] Banerjee, A., and Andrews, M. J., 2009. "3D Simulations to investigate initial condition effects on the growth of Rayleigh-Taylor mixing". *International Journal of Heat and Mass Transfer,* **52**(17), pp. 3906 – 3917.

[9] Banerjee, A., Kraft, W., and Andrews, M., 2010. "Detailed measurements of a Rayleigh-Taylor mixing layer from small to intermediate atwood numbers". *Journal of Fluid Mechanics,* **659**, pp. 129–190.

[10] Molchanov, O., 2003. "On the origin of low- and middle-latitude ionospheric turbulence". *Physics and Chemistry of the Earth,* **29**, pp. 559–567.

[11] Ebisuzaki, T., Shigeyama, T., and Nomoto, K., 1989. "Rayleigh-Taylor instability and

mixing in sn 1987a". *Astrophysical Journal,* **344**, p. L65.

[12] Colgate, S., and White, R., 1966. "The hydrodynamic behavior of supernova explosions". *Astrophysical Journal,* **143**, pp. 626–681.

[13] Gull, S., 1975. "The x-ray, optical and radio properties of young supernova remnants". *Royal Astronomical Society Monthly Notices,* **171**, pp. 263–278.

[14] Livescu, D., 2020. "Turbulence with large thermal and compositional density variations". *Annu. Rev. Fluid Mech.,* **52**, pp. 309–341.

[15] Atzeni, S., and ter Vehn, J. M., 2004. *The physics of inertial fusion: beam plasma interaction, hydrodynamics, hot dense matter*. Clarendon Press.

[16] Lindl, J., 1998. *Inertial confinement fusion: the quest for ignition and energy gain using indirect drive*. Springer, Berlin.

[17] Dimonte, G., and Schneider, M., 1996. "Turbulent Rayleigh-Taylor instability experiments with variable acceleration". *Physical Review E,* **54**, pp. 3740–3743.

[18] Livescu, D., Wei, T., and Petersen, M. R., 2011. "Direct numerical simulations of Rayleigh-Taylor instability". *Journal of Physics: Conference Series,* **318**(8), p. 082007.

[19] Ramaprabhu, P., Karkhanis, V., and Lawrie, A., 2013. "The Rayleigh-Taylor instability driven by an accel-decel-accel profile". *Physics of Fluids,* **25**, p. 115104.

[20] Aslangil, D., Livescu, D., and Banerjee, A., 2015. "Variable density mixing under variable mean pressure grtadient.". *Paper presented at the* 15^{th} *European Turbulence Conference, Delft, The Netherlands, Aug. 25-28*.

[21] Aslangil, D., Banerjee, A., and Lawrie, A., 2016. "Numerical investigation of initial condition effects on Rayleigh-Taylor instability with acceleration reversals". *Physical Review E,* **94**, p. 053114.

[22] Boffetta, G., Magnani, M., and Musacchio, S., 2019. "Suppression of Rayleigh-Taylor turbulence by time-periodic acceleration". *Phys. Rev. E,* **99**, Mar, p. 033110.

[23] Farley, Z., Aslangil, D., Banerjee, A., and Lawrie, A., 2020. "Effects of variable deceleration periods on Rayleigh-Taylor Instability with acceleration reversals". *under review Physical Review E*.

[24] Andrews, M., 1995. "Accurate computation of convective transport in transient two-phase flow". *International Journal for Numerical Methods in Fluids,* **21**, pp. 205–222.

[25] Dimonte, G., Ramaprabhu, P., and Andrews, M., 2007. "Rayleigh-Taylor instability with complex acceleration history". *Physical Review E,* **76**, p. 046313.

[26] Aslangil, D., Livescu, D., and Banerjee, A., 2020. "Effects of atwood and reynolds numbers on the evolution of buoyancy-driven homogeneous variable-density turbulence". *Journal of Fluid Mechanics,* **895**, p. A12.

[27] Aslangil, D., Livescu, D., and Banerjee, A., 2019. "Flow regimes in buoyancy-driven homogeneous variable-density turbulence". In Progress in Turbulence VIII, R. Örlü, A. Talamelli, J. Peinke, and M. Oberlack, eds., Springer International Publishing, pp. 235–240.

[28] Aslangil, D., Livescu, D., and Banerjee, A., 2020. "Variable-density buoyancy-driven turbulence with asymmetric initial density distribution". *Physica D: Nonlinear Phenomena,* **406**, p. 132444.

[29] Ramaprabhu, P., Karkhanis, V., Banerjee, R., Varsochi, H., Khan, M., and Lawrie, A., 2016. "Evolution of the single-mode Rayleigh-Taylor instability under the influence of time- dependent accelerations". *Physical Review E,* **93**, p. 013118.

[30] Richtmyer, R. D., 1960. "Taylor instability in shock acceleration of compressible fluids". *Communications on Pure and Applied Mathematics,* **13**(2), pp. 297–319.

[31] Meshkov, E. E., 1969. "Instability of the interface of two gases accelerated by a shock wave". *Fluid Dynamics,* **4**, pp. 101–104.

[32] Lawrie, A., and Dalziel, S., 2011. "Turbulent diffusion in tall tubes, part I: Models for Rayleigh-Taylor instability". *Physics of Fluids,* **23**, p. 085109.

[33] Lawrie, A., Duran-Matute, M., Scott, J., Godeferd, F., Flor, J.-B., Cambon, C., and Danaila, L., 2011. "The axisymmetric jet in a rotating reference frame". *Journal of Physics: Conference Series,* **318**, p. 032408.

[34] Atthanayake, I., Denissenko, P., Chung, Y., and Thomas, P., 2019. "Formation–breakdown cycle of turbulent jets in a rotating fluid". *Journal of Fluid Mechanics,* **868**, pp. 666–697.

[35] Lawrie, A., 2010. "Rayleigh-Taylor mixing: confinement by stratification and geometry". PhD Thesis, University of Cambridge, Cambridge, UK.

[36] Lawrie, A., and Dalziel, S., 2011. "Turbulent diffusion in tall tubes, part II: confinement by stratification". *Physics of Fluids,* **23**, p. 085110.

[37] Horne, J., and Lawrie, A., 2020. "Aspect-ratio-constrained Rayleigh-Taylor instability". *Physica D: Nonlinear Phenomena,* **406**, p. 132442.

[38] Dimonte, G., and Schneider, M., 2000. "Density ratio dependence of Rayleigh-Taylor mixing for sustained and impulsive acceleration histories". *Physics of Fluids,* **12**(2), pp. 304–321.

[39] Dimonte, G., Youngs, D. L., Dimits, A., Weber, S., Marinak, M., Wunsch, S., Garasi, C., Robinson, A., Andrews, M. J., Ramaprabhu, P., Calder, A. C., Fryxell, B., Biello, J., Dursi, L., MacNeice, P., Olson, K., Ricker, P., Rosner, R., Timmes, F., Tufo, H., Young, Y.-N., and Zingale, M., 2004. "A comparative study of the turbulent Rayleigh-Taylor instability using high-resolution three-dimensional numerical simulations: The alpha-group collaboration". *Physics of Fluids,* **16**(5), pp. 1668–1693.

[40] Wong, M. L., Livescu, D., and Lele, S. K., 2019. "High-resolution navier-stokes simulations of Richtmyer-Meshkov instability with reshock". *Phys. Rev. Fluids,* **4**, Oct, p. 104609.

[41] Andrews, M. J., and Spalding, D. B., 1990. "A simple experiment to investigate two-dimensional mixing by Rayleigh-Taylor instability". *Physics of Fluids A: Fluid*

Dynamics, **2**(6), pp. 922–927.

[42] Weber, C. R., Cook, A. W., and Bonazza, R., 2013. "Growth rate of a shocked mixing layer with known initial perturbations". *Journal of Fluid Mechanics,* **725**, p. 372–401.

[43] Thornber, B., Griffond, J., Poujade, O., Attal, N., Varshochi, H., Bigdelou, P., Ramaprabhu, P., Olson, B., Greenough, J., Zhou, Y., Schilling, O., Garside, K. A., Williams, R. J. R., Batha, C. A., Kuchugov, P. A., Ladonkina, M. E., Tishkin, V. F., Zmitrenko, N. V., Rozanov, V. B., and Youngs, D. L., 2017. "Late-time growth rate, mixing, and anisotropy in the multimode narrowband Richtmyer–Meshkov instability: The θ-group collaboration". *Physics of Fluids,* **29**(10), p. 105107.

[44] Ramaprabhu, P., and Andrews, M. J., 2004. "Experimental investigation of Rayleigh-Taylor mixing at small atwood numbers". *Journal of Fluid Mechanics,* **502**, p. 233–271.

NOMENCLATURE

A Atwood number

α Rayleigh-Taylor instability mixing layer self-similar growth constant

B_{33} Vertical anisotropic tensor

f_h The mass fraction of the pure heavy fluid

f_l The mass fraction of the pure light fluid

g The acceleration field

h_b Bubble heights

h_s Spike heights

ρ_h The density of the pure heavy fluid

ρ_l The density of the pure light fluid

θ Richtmyer-Meshkov instability mixing layer self-similar growth exponent

Θ The molecular mixing parameter

W Integral width of mixing layer

W^* Normalized mixing layer width

AD Accel - Decel

ADA Accel - Decel - Accel

AZ Accel - Zero gravity

AZA Accel - Zero gravity - Accel

CG Constant gravity

HVDT Homogeneous Variable-Density Turbulence

ILES Implicit Large Eddy Simulation

KE Kinetic Energy

PE Potential Energy

RMI Richtmyer-Meshkov Instability

RTI Rayleigh-Taylor Instability

LIST OF FIGURES

LIST OF TABLES

Table 1: The presented cases that includes the Constant Gravity (CG), Accel-Decel (AD), Accel-Zero gravity (AZ), and Accel-Zero gravity-Accel (AZA) cases.

Case ID	First Reversal Instant (s)	Second Reversal Instant (s)
CG	NA	NA
AD	2	NA
AZ	2	NA
AZA1	2	3.7
AZA2	2	4.35
AZA3	2	6
AZA4	2	10

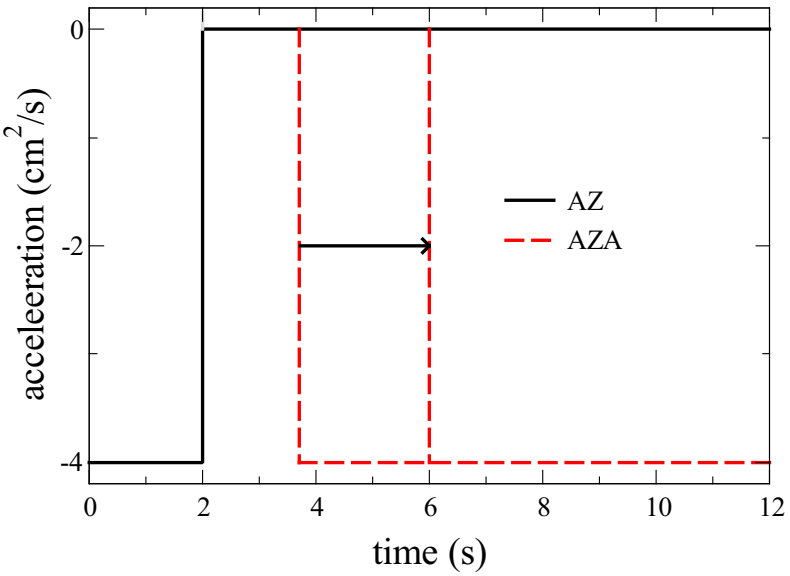

Fig. 1: Acceleration profile for the different cases.

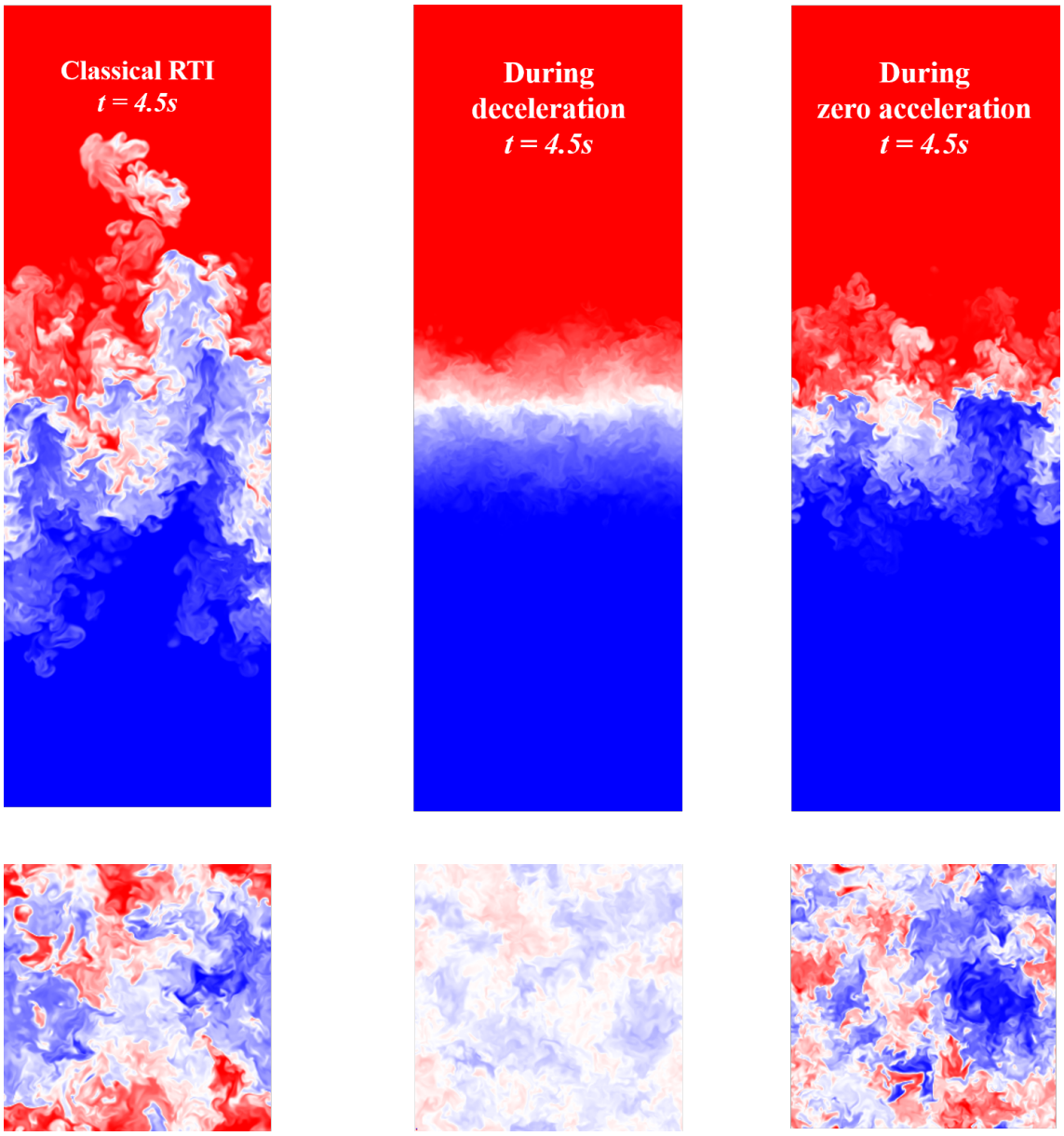

Fig. 2: 2-D vertical (on top row) and horizontal (on bottom row) density field for the CG, AD, and AZ cases at $t = 4.5s$. The red color and blue colors represent pure heavy ($\rho_h = 3g/cm^3$) and light ($\rho_h = 1g/cm^3$) fluids respectively, and white color represents the fully-mixed flow ($\rho = 2g/cm^3$). Please note that there are no dark blue and red color within the horizontal slice of the density field for the AD case as the flow is mostly mixed at the interface with the local maximum and minimum values $1.66g/cm^3$ and $2.24g/cm^3$. The AD data is taken from a case examined further in [23].

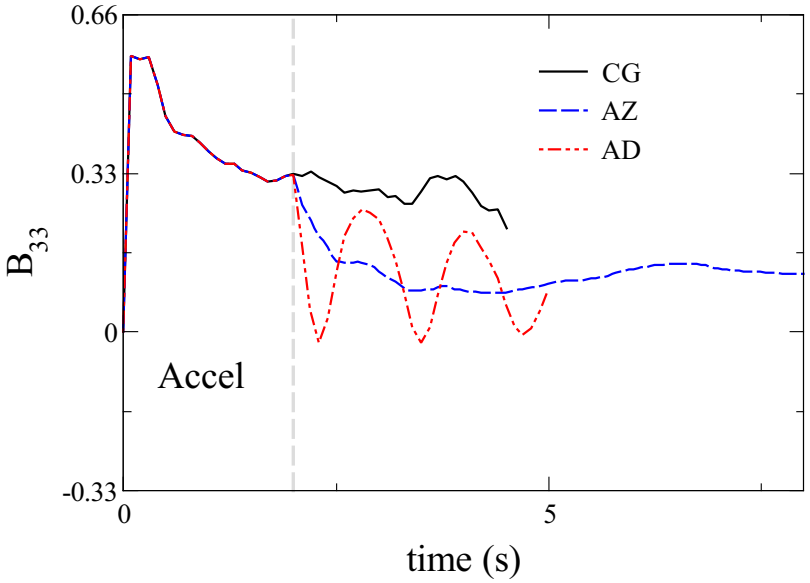

Fig. 3: The time evolution of the vertical anisotropic tensor (B_{33}) for the CG and AZ cases. The AD data is taken from [23].

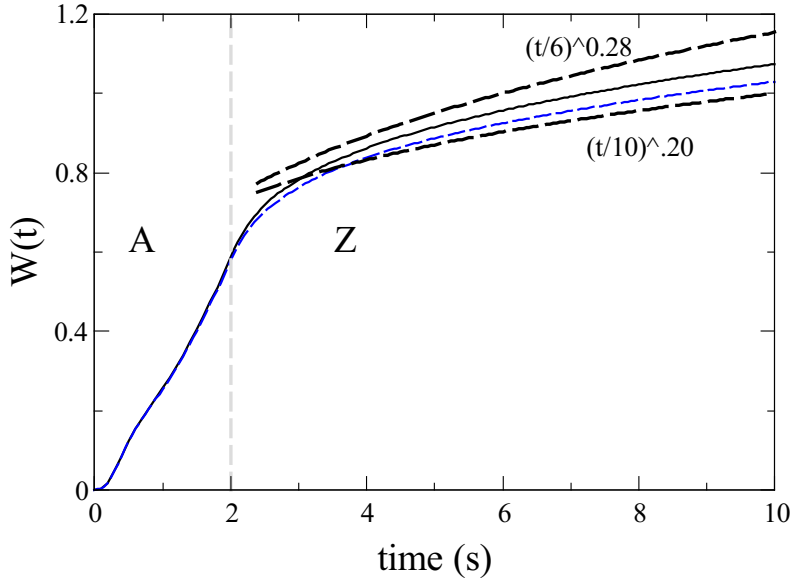

Fig. 4: The time evolution of the mixing layer width of the Rayleigh-Taylor instability ($W(t)$) for the CG, AZ1 and AZ2 cases. The dashed-black lines represents the exponential growth rates $(t/6)^{0.28}$ and $(t/10)^{0.20}$ of the mixing layer width.

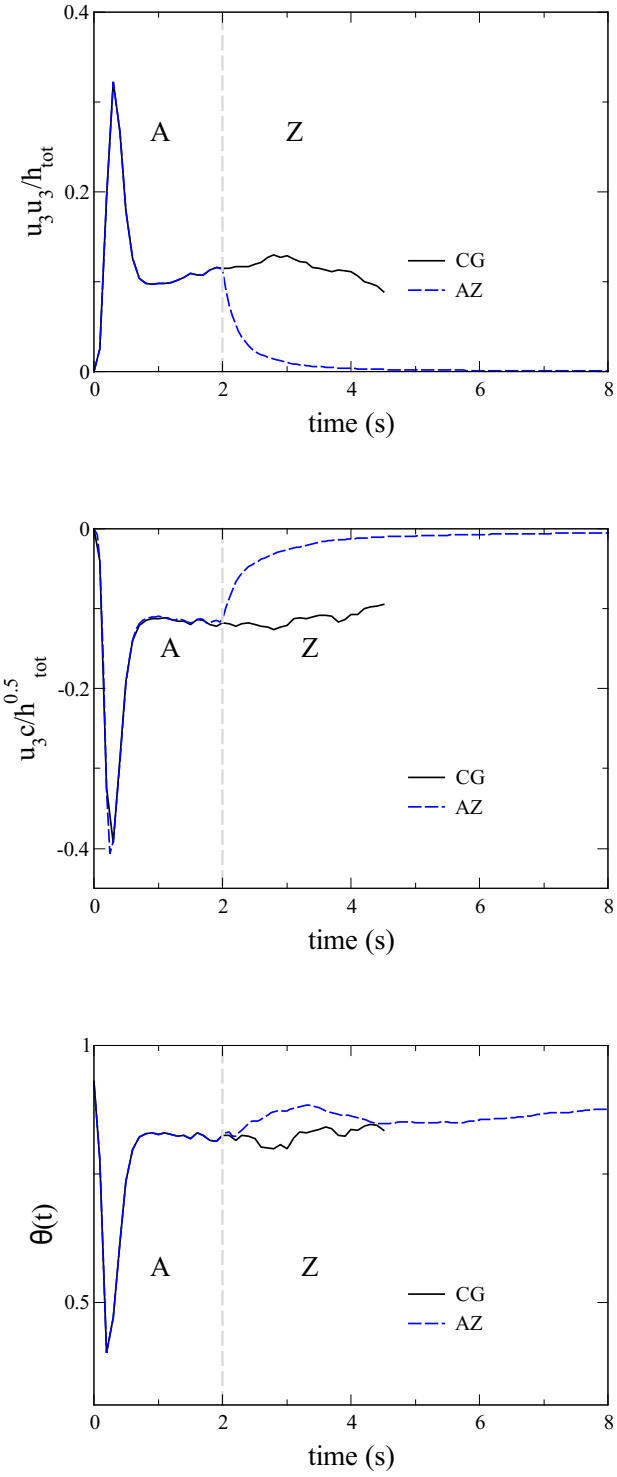

Fig. 5: The time evolution of (a) the normalized density-velocity correlation ($\frac{u_3 u_3}{h}$), (b) the normalized density-velocity correlation ($\frac{u_3\, c}{h^{0.5}}$), and (c) the mixing parameter (θ) for the CG and AD cases.

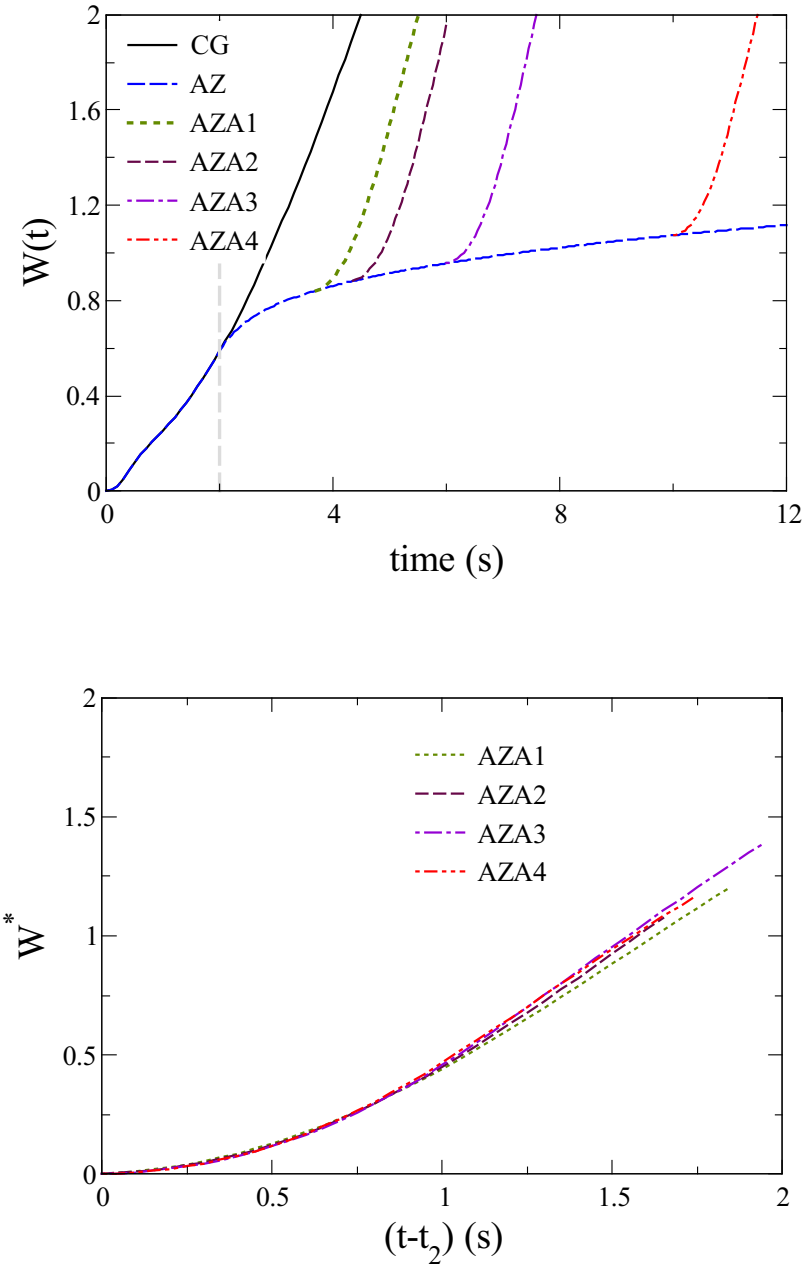

Fig. 6: The time evolution of (a) the mixing layer width of the Rayleigh-Taylor instability ($W(t)$) for the all cases, (b) the normalized mixing layer width of the Rayleigh-Taylor instability ($W^*(t) = W(t) - W(t_2)$).

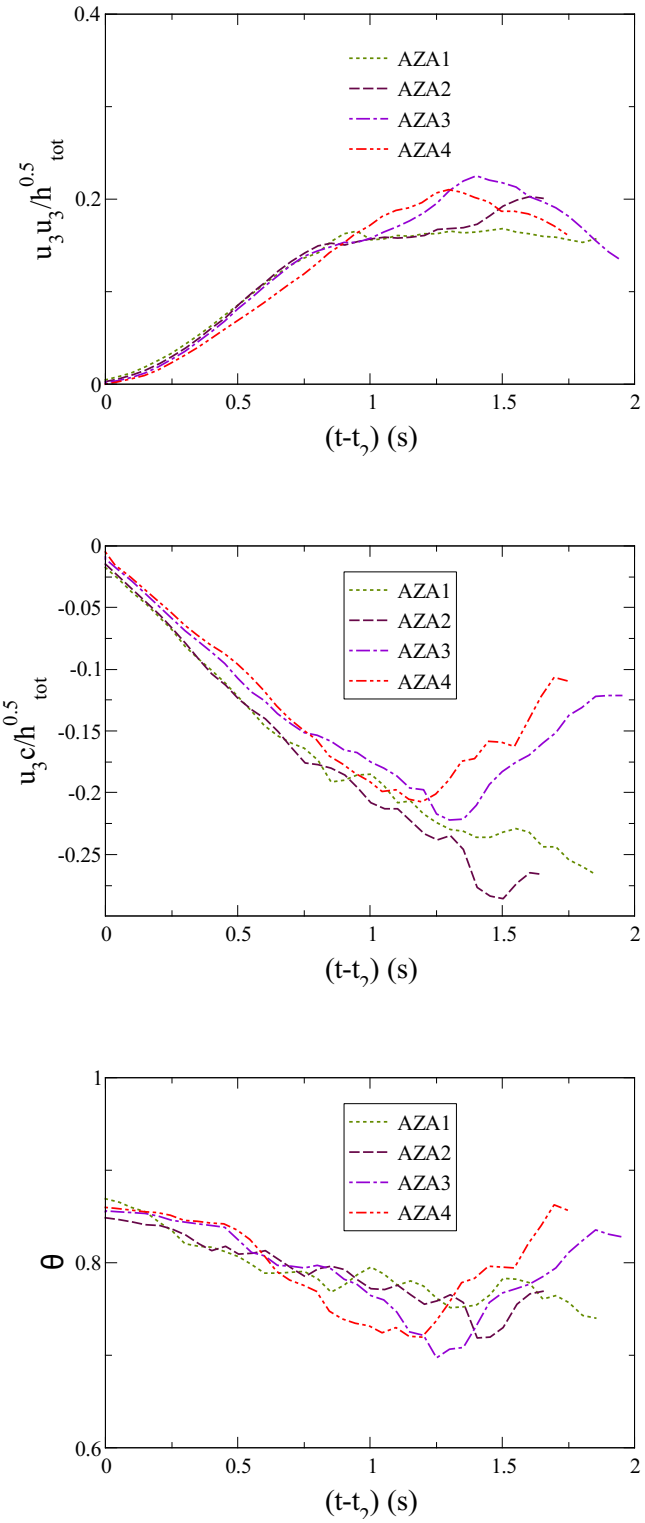

Fig. 7: The time evolution of (a) the normalized density-velocity correlation ($\frac{u_3 u_3}{h}$), (b) the normalized density-velocity correlation ($\frac{u_3\ c}{h^{0.5}}$), and (c) the mixing parameter (θ) for the AZA cases.

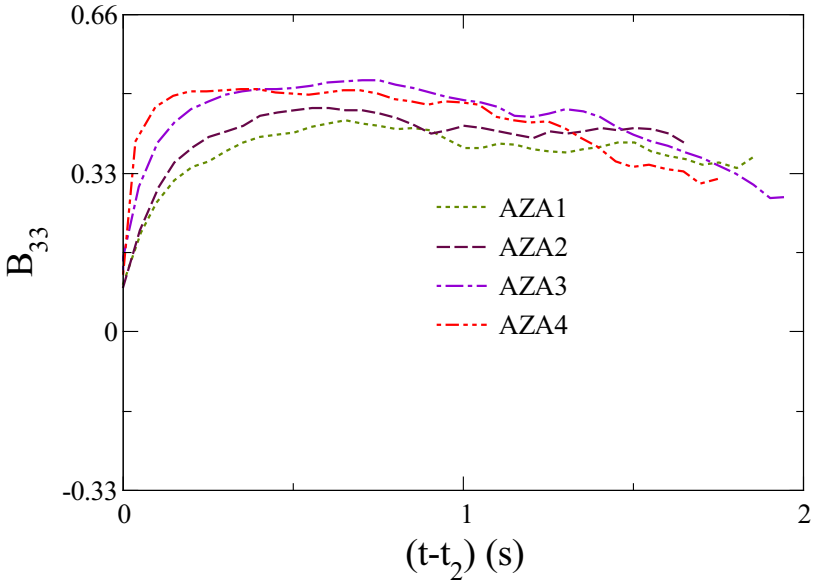

Fig. 8: The time evolution of the vertical anisotropic tensor (B_{33}) for the AZA cases.